Nnamchi et al., *Cogent Engineering* (2019), 6: 1657264
https://doi.org/10.1080/23311916.2019.1657264

cogent engineering

MECHANICAL ENGINEERING | RESEARCH ARTICLE

Experimental verification of suitability of insulation testing rig in determining thermophysical properties of insulating materials

S. N. Nnamchi[1]*, O. A. Nnamchi[2], O. S. Odebiyi[1], O. O. Edosa[1] and T. Wanazusi[1]

Received: 27 June 2019
Accepted: 14 August 2019
First Published: 20 August 2019

*Corresponding author: S. N. Nnamchi, Mechanical Engineering, Kampala International University, Ggaba Road, Kansanga, P.O.B, Kampala 20000, Uganda
E-mail: stephen.nnamchi@kiu.ac.ug

Reviewing editor:
Duc Pham, School of Mechanical Engineering, University of Birmingham, UK

Additional information is available at the end of the article

Abstract: Verification of suitability of insulation testing rig (ITR) in determining the thermophysical properties of insulating materials (IM) is strongly based on the measurement of temperatures on the inner/outer surfaces of the insulators (white cotton fabric, molded ash, molded rice husk and molded sawdust), outer surface of mild steel, and the temperatures of the external/internal heat transfer fluids (air/water). The dimensionless excess temperature (heat rejection factor(HRF)) was determined as the ratio of IM to mild steel excess temperature. Thermal balance on the IM led to mechanistic thermal equation whose coefficient yielded the insulation parameter, which is synonymous with the fin parameter. The thermal conductivity of the insulators was uniquely determined as a function of HRF, geometric shapes of the insulator/mild steel, and the internal/external fluid properties. Distinctively, the thermal diffusivity was determined as function of rate of dimensionless excess temperature and the insulation parameter rather than as ratio of thermal conductivity to thermal storage capacity. Essentially, the thermal conductivity determined for the above-mentioned IM were;

ABOUT THE AUTHOR

S. N. Nnamchi is a Senior Lecturer in Mechanical Engineering Department (MED), Kampala International University (KIU), Uganda. He holds PhD (2014) in Mechanical Engineering (Thermofluids) from UNIPORT. He specializes in renewable/thermal systems; design, modelling, and simulation. Essentially, this work advances development of insulating materials and addition of chain-value to agricultural wastes.
O. A. Nnamchi is a postgraduate student of Bioprocess and Food Engineering in the Department of Agricultural Engineering and Bio Resources, MOUA. She holds B.Eng (Chemical, 2005) from FUTOW. She is experienced in material characterization.
O. S. Odebiyi is a lecturer in MED, KIU, Uganda. He holds M. Sc. (Mechanical, 2016) from UNILAG. His research interests include material development/mechanical design.
O. O. Edosa is a Lecturer in MED, KIU, Uganda. He holds M.Eng (Mechanical design, 2014) from UNILAG. He is experienced in material development, manufacturing/mechanical design.
T. Wanazusi is an undergraduate student in MED, KIU, Uganda.

PUBLIC INTEREST STATEMENT

ITR is a feasible and low cost equipment for determining the thermal properties (TP) of powdered materials enveloped in a thermally known material. TP is useful in developing and selecting raw materials for insulation purposes. This equipment has the ability to track both the historic and spatial excess temperature of a material. Superficially, it gives the heat rejection factor (HRF); the preliminary TP of a material. The thermal conductivity (TC) is fathomed by engaging the HRF, geometry of the materials and surrounding fluid conditions. The TC is in-built in the excess temperature coefficient (insulation parameter, IP) another eye-opener to the TC of materials. The IP is useful in estimating the thermal diffusivity, TD of a material (ratio of TC to thermal storage capacity). Thus, a material of low; HRF, TC, TD and high IP is ideal for insulation. A unification of the TP cannot lead to erroneous characterisation of materials.

0.0597, 0.0377–0.0555, 0.0251–0.0344 and 0.0110–0.0293 W/mK, respectively. The thermal diffusivity obtained for the aforementioned IM were; 3.443, 1.3008–1.9302, 1.0384–1.4418 and 0.2499–0.8384 m^2/s, respectively. The empirical results produced the numerical values of the four cardinal thermophysical properties, which unanimously agreed with the established results in literature. This agreement substantiates the fact that ITR is quite suitable in determining the thermophysical properties of future insulators. Therefore, this study strongly endorses the application of ITR for characterization and development of fibrous agricultural wastes as insulators.

Subjects: Engineering & Technology; Engineering Education; Mathematics & Statistics for Engineers; Mechanical Engineering; Materials Science; Electronic Devices & Materials

Keywords: experimental verification and heat transfer; composite/monolithic insulating materials; heat rejection factor; insulation parameter; thermal conductivity and diffusivity; insulation testing rig

1. Introduction

Global campaign on waste to chain-value addition is of paramount interest in eco-environmental sustainability. Thus, conversion of fibrous agricultural wastes (A-wastes) into insulating materials (IM), helps to protect our environment and equally reduces the cost of advanced IM as dependence on them is highly minimized.

Typically, high and low density solid materials are poor and good thermal IM, respectively. Commensurately, solid materials of extremely low density are characterized by very low thermal conductivity, which qualifies them as IM. Likewise, solid material of tremendous low thermal conductivity corresponds to remarkable low thermal diffusivity, specific heat capacity and density, which constitutes a second criterion for the selection of IM (Guo & Feng, 2011; Stabler et al., 2018).

Additionally, solid materials with very high insulation parameter (analogous to fin parameter) are likely to be characterized with low thermal conductivity, which distinguishes them as good IM. Besides, solid materials with diminutive heat rejection factor (HRF) probably possess a low thermal conductivity, thermal diffusivity, and density, thus, they are potential IM (Balaguru & Jeyaprakash, 2019). Therefore, insulation parameter and HRF could serve as additional criteria for future selection of IM.

Pertinently, Nnamchi, Nnamchi, Sangotayo, Mundu, and Edosa (2019) and Yüksel (2016) have reviewed variants of the equipment employed in the characterization and development of IM; a flow meter, guarded heat flow meters, guarded hot plate instrument, flash diffusivity methods, calibrated hot box, etc. Basically, they function on the principle of heat transfer from a known heat source to a heat sink. Traditionally, the thermal flux exposed to the insulating material is quantified from the measured voltage and current. The thermal conductivity is then estimated based on Fourier first law of thermal conduction (Kreith, 2000; Oko, 2011; Schilling, Zhang, & Bossen, 2019; Zhu, Wu, Chen, & Ren, 2018). The thermal diffusivity of an insulating material is determined as the ratio of its thermal conductivity to thermal storage capacity of the insulating material (Behnia & Kapitulnik, 2019; Oko, 2008; Rajput, 2007).

Appropriately, Uzun (2014) carried out measurements of thermal conductivity and other related thermophysical properties of woven fabric with an Alambeta instrument (Sensora Instruments), which is capable of measuring; the thermal diffusion, thermal conductivity, thermal resistance, and thermal absorption-specific thickness of fabric IM. Moreover, he recorded a thermal conductivity of 0.341 W/mK based on experimentation. Also, Uzun (2014) provided thermal diffusivity of woven fabric as ratio of thermal conductivity to thermal storage capacity (which is equivalent to the product of density and specific heat capacity of the insulating material); with accompanying results; 0.86–3.41 m^2/s.

Consistently, Ayugi, Banda, and D'Ujanga (2011) employed a hot wire equipment (Quick thermal conductivity meter) in the measurement of arbitrary thickness of local IM (clay: 0.184–0.219, kaolin: 0.466–0.544, ash: 0.276–0.338, banana fibers: 0.185–0.240, sugarcane fibers: 0.086–0.107, sawdust: 0.185–0.240 and charcoal dust: 0.1840–0.219 $Wm^{-1}K^{-1}$) such that heat loss to the surrounding at 25 °C is minimized. They used transient heat pulse method to generate the temperature history at the interval of 30 s on a separate sample of the specimen to determine the thermal diffusivity of materials (clay: 1.58, kaolin: 4.27, ash: 3.67, banana fibers: 8.13, sugarcane fibers: 5.05, sawdust: 1.12 and charcoal dust: 6.09 m^2s^{-1}).

Furthermore, Kyauta, Dauda, and Justin (2014) produced a molded rice husk with thermophysical properties (thermal conductivity: 0.1961–0.2660 W/mK, dependable property: 22.114 m^{-1}). They utilized P.A Hilton Thermal Conductivity Apparatus in determining the thermal conductivity of the molded insulating material, which requires a cold sink.

Additionally, Karthikeyan, Manapparai, Prabu, and Ekanthamoorthy (2018) used a cylindrical thermal conductivity apparatus specialized for powdered IM in their experiments. They measured the thermal conductivity of sawdust powder and recorded thermal conductivity of 0.030–0.220 W/mK for the inner (outer) temperature range of 50(47)–70(58 °C). Moreover, Sreenarayanan and Chattopadyay (1986) carried out similar experiment as Uzun (2014) for the rice husk insulating material and recommended thermal diffusivity of 0.934–1.210 m^2/s.

Essentially, Engineers Edge (2019) presents the thermal diffusivity of pure sawdust as 0.82×10^{-7} m^2/s, However, the technique deployed in determining the value of thermal diffusivity for ash is anonymous. Contrarily, Ebiega (2017) and Ayugi et al. (2011) applied the same technique of using the ratio of thermal conductivity to thermal storage capacity of the insulating material to establish a value of 3.67×10^{-7} m^2/s.

Conversely, Kuye, Oko, and Nnamchi (2010) have presented the thermophysical properties of ground neem seed based on measurement of the temperature history of the ground neem seed in conjunction with the inverse problem method, which is integrally pivoted on the Levenberg-Marquardt algorithm (Ozisik, 1993) in establishing the thermal conductivity of the ground neem seed. However, the thermal diffusivity was computed as the popular ratio of thermal conductivity to thermal storage capacity of the ground neem seed in accordance to Uzun (2014), Ayugi et al. (2011), Kyauta et al. (2014), Karthikeyan et al. (2018), and Sreenarayanan and Chattopadyay (1986).

Innovatively, the present work will employ an insulation-testing rig (ITR) in determining the thermophysical properties of molded insulation powders. The ITR has unique capacity to produce the excess temperature history of molded IM both in space and time by the virtue of its projected cylindrical test surface. Besides, the classical thermophysical properties (thermal conductivity and thermal diffusivity) of the IM, which are used to confirm their suitability for insulation. Extraordinarily, the present technique introduces additional thermophysical properties to consolidate the verification of A-wastes as future IM. These veritable thermophysical properties are the HRF (dimensionless excess temperature) and insulation parameter. The HRF is a fraction of the thermal energy an insulating material is unable to be conserved; it is proposed to be a function of distance along the cylindrical test surface of the ITR. The insulation parameter is a dimensional parameter akin to fin parameter; it is thermal coefficient of linear excess temperature in thermal transport equation describing the heat flow through the IM. Mathematically, it is the ratio of the product of forced convective heat transfer coefficient and the perimeter of an insulating material to the product of the thermal conductivity and cross-sectional area and of an insulating material available to conductive thermal flux. Hence, the present work is bound to use the four thermophysical criteria in recommending A-wastes as potential insulating material or not.

Therefore, the present work is set to experimentally determine the four thermophysical properties of A-wastes IM; the HRF, thermal conductivity, insulation parameter and thermal diffusivity of

the selected A-waste materials. Furthermore, to compare the experimentally derived results with the established literature results to fathom the suitability of ITR in testing the thermophysical properties of A-wastes.

2. Materials and methods

The proposed state of the art requires availability of the following materials: an ITR, digital multimeters (thermocouples), weighing scale, Vernier caliper, measuring tape, stop watch, electrical heater, marker and cable ties for the experimentation; formulation of mathematical model and simulation of thermal fluxes (conductive and convective) around the cylindrical test surface of the ITR.

2.1. Construction of insulating material mold and slab

The outer diameter of cylindrical mild steel surface (CMSS) of the ITR was gauged with a stainless steel Vernier caliper to measure its diameter. Then, the working thickness of the insulating material (IM) was added to the radius of CMSS to obtain the radius of IM and subsequently the diameter of the IM. The perimeter of the insulating material was calculated by multiplying its diameter, D_i with pi (π), which corresponds to the width of the insulating material mold (IMM). The working thickness is equivalent to the height of IMM whereas the length of the IM (l_i) is commensurate to the length of the CMSS. The IMM is simply represented in Figure 1.

The slab in Figure 1 was developed by binding the pulverized insulating material with a light glue in Figures 2 and 3. A white cotton fabric (WCF) was laid and the bonded insulating material was filled to the brim of the IMM and rammed to compact well. Subsequently, the slab was laid on a cylindrical surface to aid it in maintaining its curvature while setting and later the set composite was laid on the cylindrical surface of ITR to dry for a period of 21 days prior to the experiments.

2.2. Experimentation

The cylindrical surface of the ITR was fitted with five UNI-T (UT33C+) and one Allsun (EM420A) digital multimeters (thermocouples) to measure the spatial temperature distribution along the cylindrical surface, while the seventh thermocouple, UNI-T (UT33C+) was permanently inserted into the finned bath for measuring temperature of the interior working fluid (water), whereas the eighth and last multimeter UNI-T (UT33C+ thermocouple) was used to measure the temperature of an external working fluid (air).

A stainless Vernier caliper (Tokyo) was used to gauge the diameter of the cylindrical surfaces. The measuring tape (AMS56 50m Tape measure) and marker (MK-MP10) was used to calibrate temperature measuring points. The tips of the multimeter were fastened on the cylindrical surface with the aid of cable ties (NT 0430-48-BK). The experimental data were logged while cooling the heated ITR. Temperature was recorded on three minutes interval for a period of 1.30 h (≈ 1 h 18 min). The experimental setup is pictorially represented in Figure 4. Finally, CAS digital scale (150 kg, EB-300) was used to weigh the WCF alone, WCF used in the composite and the weight of the dried composite.

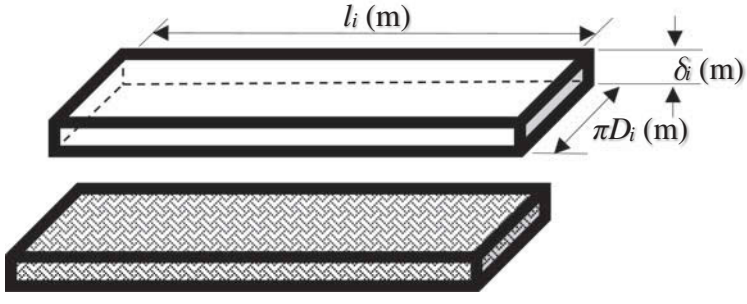

Figure 1. An insulating material mold with a molded slab.

(a) White cotton fabric, glue and ash

(b) White cotton fabric glue and rice husk

(c) white cotton fabric, glue and sawdust

Figure 2. Development of composite insulating materials.

Figure 3. Developed composite insulating materials.

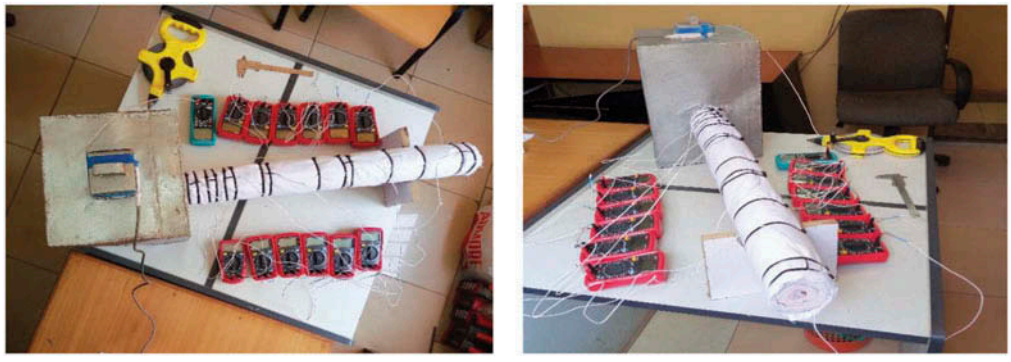

Figure 4. Insulation testing rig wrapped with white cotton fabric insulating material.

2.3. Mathematical formulation

Considering energy balance around the cylindrical differential volume in Figures 5 and 6; the component energy balance equation is formulated on the composite materials or monolithic insulating material (*i*).

Conventionally, the excess temperature varies both in space (x-axis) and time; which is temperature difference between the insulating material and surrounding fluid (air at ambient condition).

The thermal flux in the differential volume is made up of conductive thermal flux (Q_x) which flows in the direction perpendicular to the cross sectional area of both insulating material and the

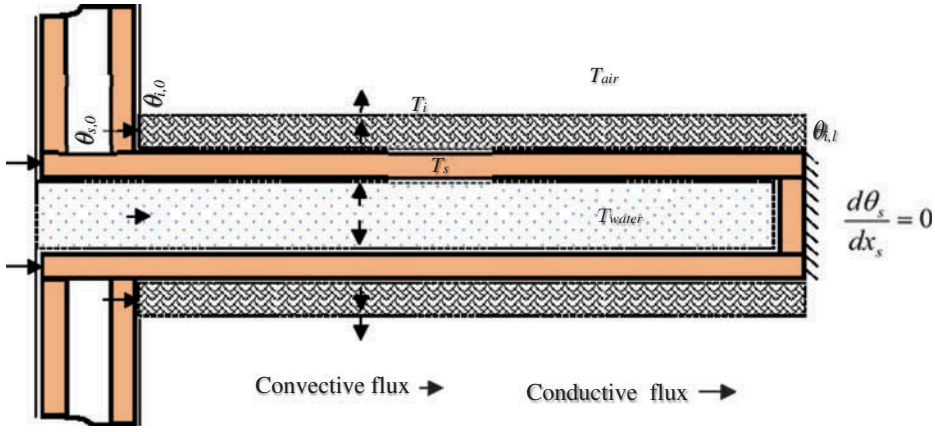

Figure 5. Vectorial representation of heat flux on the insulating material (i) and mild steel pipe (s) of an insulation testing rig.

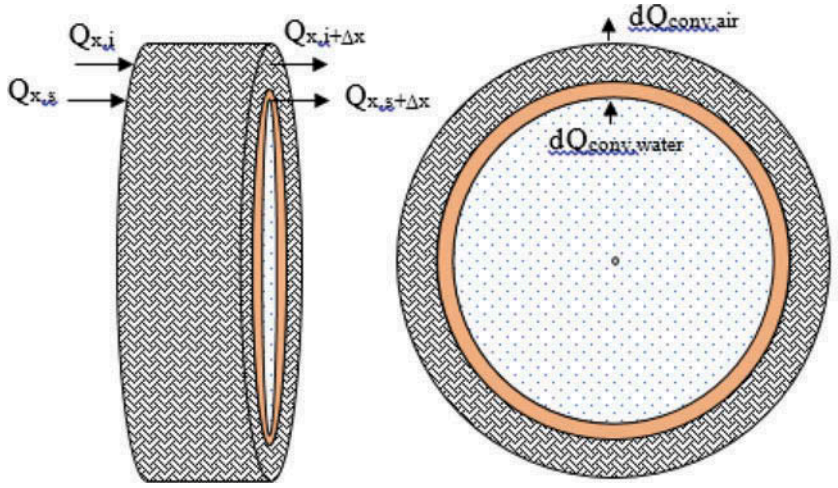

Figure 6. The differential volume of thermal flux on the insulating material (i) and mild steel pipe (s).

mild steel pipe whereas the convective flux (dQ) flows perpendicular to the curved surface area of both insulating material and mild steel test surface.

The unsteady state excess temperature balance along the IM is expressed in Equation (1) as follows:

$$\textit{Energy accumulation within the insulating material} = \textit{energy input across the insulating material} - \textit{energy output across the insulating material} \tag{1}$$

Thus, the thermal balance on the insulating material (*i*) is expressed in Equations (2) and (3) as follows:

$$A_{c,i}\,\rho_i cp_i \frac{\partial \theta_i}{\partial t} = k_i A_{c,i} \frac{\partial^2 \theta_i}{\partial x_i^2} - h_a P_{i,out}\,\theta_i \tag{2}$$

where

$$\theta_i = T_i - T_a \tag{3}$$

where $A_{c,i}$ *(m^2)* is the cross sectional area of the insulating material available to the conductive thermal flux, θ_i *(K)* is the excess temperature along the insulating material, ρ_i *(kg/m^3)* is the density of the insulating material, cp_i *(kJ/kgK)* is the specific heat capacity of the insulating material, *t (s)* is

the time dependency of the excess temperature, k_i *(W/mK)* is the thermal conductivity of the insulating material, x_i *(m)* is the space dependency of the excess temperature, h_a *(W/m^{2}K)* is the convective heat transfer coefficient between the insulating material at T_i *(K)* and ambient at T_a *(K)*, $P_{i,o}$ *(m)* is the perimeter of the insulating material available to convective heat flux, T_i is the temperature of the insulating material.

Solving Equation (2) at unsteady state condition by the method of additive separation in Equation (4a)

$$\theta(x,t) = \phi(t) + \psi(x) \tag{4a}$$

and integrating factor for the initial condition, $\theta_i(x_i,0) = \theta_{i,0}\ \forall \quad 0 \le x_i \le l_i$ results in time- dependent excess temperature, $\phi(t)$ in Equation (4b).

$$\phi(t) = \theta_{i,0}\, e^{-\alpha_i m_i^2 t} + \frac{\lambda_i^{\Gamma}}{m_i^2}\left(1 - e^{-\alpha_i m_i^2 t}\right); \tag{4b}$$

$$i = \{1,2,3,4\} = \{\text{white cotton fabric (WCF), WCF} \cup \text{ash, WCF} \cup \text{sawdust, WCF} \cup \text{rice husk}\}$$

Rearranging Equation (4b) leads to Equation (5) an explicit expression for the thermal diffusivity, α_i of the IM

$$\alpha_i = \frac{-1}{m_i^2 t}\ln\left(\frac{\theta_i(t) - \lambda_i^{\Gamma}/m_i^2}{\theta_{i,0} - \lambda_i^{\Gamma}/m_i^2}\right) = \frac{k_i}{\rho_i cp_i}; \tag{5}$$

$$i = \{1,2,3,4\} = \{\text{white cotton fabric (WCF), WCF} \cup \text{ash, WCF} \cup \text{sawdust, WCF} \cup \text{rice husk}\}$$

In the same vein, solving Equation (2) by the method of additive separation; the specific solution of the space term (the boundary value problem) is obtained by seeking the homogeneous solution and particular solution (via method of undetermined coefficients) of the space-dependent term, $\psi_i(x)$

$$\psi_i(x) = \theta_{\text{homogeneous}}(x) + \theta_{\text{particular}}(x) \tag{6a}$$

for the boundary conditions; $\theta_i(0,t) = \theta_{i,0}$, $\theta_i(l,t) = \theta_{i,l}\ \forall \quad t>0$ yields the space-dependent solution, $\psi_i(x)$ in Equation (6b).

$$\begin{aligned}\psi_i(x) = {} & \frac{\theta_{i,0} - \theta_{i,l}e^{m_i l} - \left(\lambda_i^{\Gamma}/m_i^2\right)\left(e^{m_i l} - 1\right)}{1 - e^{2m_i l}} e^{m_i x_i} \\ & + \frac{\theta_{i,0} - \theta_{i,l}\, e^{-m_i l} - \left(\lambda_i^{\Gamma}/m_i^2\right)\left(e^{-m_i l} - 1\right)}{1 - e^{-2m_i l}} e^{-m_i x_i} - \frac{\lambda_i^{\Gamma}}{m_i^2}\end{aligned} \tag{6b}$$

$$i = \{1,2,3,4\} = \{\text{whitecottonfabric(WCF), WCF} \cup \text{ash, WCF} \cup \text{ sawdust, WCF} \cup \text{rice husk}\}$$

According to Rajput (2007), the rate of heat transfer through the IM, $Q_{i,j}$ (W) balances the product of rate of heat transfer through the mild steel pipe, $Q_{s,j}$ (W) and fraction of heat loss from the IM to the surrounding, $n_{i,j}$ (-) in Equation (7) as follows:

$$\frac{1}{N}\sum_{j=1}^{N=6} Q_{i,j} = \frac{1}{N}\sum_{j=1}^{N=6} n_{i,j} Q_{s,j}\ ; \quad j = 1,\ 2,\ \cdots, 6; \tag{7}$$

$$i = \{1,\ 2,\ 3,\ 4\} = \{\text{white cotton fabric (WCF), WCF} \cup \text{ash}\prime, \text{ WCF} \cup \text{sawdust}\prime, \text{ WCF} \cup \text{ricehusk}\prime\}$$

Also, the thermal conductivity, $k_{i,j}(W/mK)$ of the IM is defined in Equation (8) as follows:

$$\sum_{j=1}^{N=6}\left(\frac{1}{r_{s,in}h_w}+\frac{\ln\left(r_{s,out}/r_{s,in}\right)}{k_{s,j}}+\frac{\ln\left(r_{i,out}/r_{i,in}\right)}{k_{i,j}}+\frac{1}{r_{i,out}h_a}\right)^{-1}$$
$$=\sum_{j=1}^{N=6}n_{i,j}\left(\frac{1}{r_{s,in}h_w}+\frac{\ln\left(r_{s,out}/r_{s,in}\right)}{k_{s,j}}+\frac{1}{r_{s,out}h_a}\right)^{-1} \tag{8}$$

The thermal rejection factor, $n_{i,j}$ is fitted as the function of the distance, x along the ITR test surface in Equation (9)

$$n_{i,j}=f\left(x_j\right);\qquad j=1,\,2,\,\cdots,\,6 \tag{9}$$

The average thermal conductivity, $\bar{k}$ of the IM is given in Equation (10)

$$\bar{k}_i=\frac{1}{N}\sum_{j=1}^{N=6}k_{i,j}=\frac{1}{N}\sum_{j=1}^{N=6}\frac{n_{i,j}\,\ln\left(r_{i,out}/r_{i,in}\right)}{\left(1-n_{i,j}\right)\left(\frac{1}{r_{s,in}h_w}+\frac{\ln\left(r_{s,out}/r_{s,in}\right)}{k_{s,j}}+\frac{1}{r_{s,out}h_a}\right)};\qquad j=1,\,2,\,\cdots,\,6 \tag{10}$$

The steady state insulation parameter, $m_i(1/m)$ for the IM is defined in Equation (11) as follows:

$$m_i^2=\frac{h_aP_{i,out}}{A_{c,i}\bar{k}_i}; \tag{11}$$

The Eigenvalue, $\lambda_{i,m}\,;\,m=1,\,2,\,\ldots,\,\infty$ in Equation (12) is obtained by transcendental equation (Ozisik, 1993) for the boundary conditions specified in Figure 5 is expressed in Equation (12) as

$$\lambda_{i,m}\tan\left(\lambda_{i,m}l_i\right)=\frac{h_{so,bath}}{\bar{k}_i}; \tag{12}$$

The thermal conductivity of the composite (wcf + glue, g + powder, p), $k_{wcf+g+p}(W/mK)$ and molded powder, $k_{g+p}(W/mK)$ is defined in Equation (13).

$$k_i=k_{wcf+g+p}=\frac{\omega_{wcf}k_{wcf}+\omega_{g+p}k_{g+p}}{\omega_{wcf}+\omega_{g+p}}\;\;k_{g+p}=\frac{k_{wcf+g+p}-\omega_{wcf}k_{wcf}}{\omega_{g+p}};\;\;k_{g+p}=\frac{k_{wcf+g+p}-\omega_{wcf}k_{wcf}}{\omega_{g+p}} \tag{13}$$

Similarly, the thermal diffusivity of the composite, $\alpha_{wcf+g+p}$ and molded powder, $\alpha_{g+p}(\mathrm{m}^2/\mathrm{s})$ is proposed in Equation (14).

$$\alpha_i=\alpha_{wcf+g+p}=\frac{\omega_{wcf}\alpha_{wcf}+\omega_{g+p}\alpha_{g+p}}{\omega_{wcf}+\omega_{g+p}}\;\;\alpha_{g+p}=\frac{\alpha_{wcf+g+p}-\omega_{wcf}\alpha_{wcf}}{\omega_{g+p}} \tag{14}$$

The thermal effectiveness or thermal retention factor, $\varepsilon_{th,i}$ of the IM is determined by thermodynamic relation in Equation (15).

$$\varepsilon_{th,i}\approx 1-\frac{\theta_{i,out}}{\theta_{i,in}};\quad\theta_{i,in}=\theta_{s,out} \tag{15}$$

$$i=\{1,\,2,\,3,\,4\}=\{\text{whitecottonfabric(WCF)},\;\text{WCF}\cup^{\text{ash}}\prime,\text{WCF}\cup^{\text{sawdust}}\prime,\text{WCF}\cup\{\text{ricehusk}\prime\}$$

2.3.1. Computation of parameters and TP of heat transfer fluids

The perimeter of the inner and outer surfaces of the insulating material is defined in Equation (16)

$$P_{i,out}=\pi\qquad D_{i,out}P_{i,in}=\pi D_{i,in} \tag{16}$$

whereas the diameter (D) of the inner and outer surfaces of the insulating material is well-defined in Equation (17)

$$D_{i,out}=2\left(r_{i,out}+\delta_i\right)\qquad D_{i,in}=2r_{i,in}=2r_{s,out} \tag{17}$$

The cross sectional area available to conduction flux in the insulating material is given in Equation (18) as

$$A_{c,i} = \frac{\pi}{4}\left(D_{i,out}^2 - D_{i,in}^2\right) \tag{18}$$

According to Nnamchi, Sanya, Zaina, and Gabriel (2018) and Nnamchi et al. (2019) the external heat transfer coefficient over the insulating material is expressed in Equation (19) as

$$h_{air} = \frac{k_{air}}{D_{i,out}}\left(0.193\,\mathrm{Re}_{D_{i,out}}^{0.618}\,\mathrm{Pr}^{1/3}\right) \;\exists\;\; \mathrm{Pr} \geq 0.70,\;\; 4000 \leq D_{i,out} \leq 40000 \tag{19}$$

and the internal heat transfer coefficient over the insulating material is expressed in Equation (19) as

$$h_w \approx \frac{k_w}{D_w}\left\{0.60 + \frac{0.387Ra_{D_w}^{1/6}}{\left[1+(0.559/\mathrm{Pr})^{9/16}\right]^{8/27}}\right\}^2 \;\; for \;\; 10^{-1}<Ra_{D_w}<10^{12},$$
$$Ra_{D_w} = Gr_{D_w}\mathrm{Pr}_w;\;\; Gr_{D_w} = \frac{g\,(D_w)^3\beta\,(T_w - T_i)}{\mu^2/\rho^2},\;\; \mathrm{Pr} = \frac{\mu_w\, cp_w}{k_w} \tag{20}$$

Also, the convective heat transfer coefficient around the bath is given in Equation (21) (Nnamchi et al., 2019, 2018) as follows:

$$h_{so,bath} \approx \frac{k_a}{l_{s,o}}\left\{0.825 + \frac{0.387Ra_{l_{s,out}}^{1/6}}{\left[1+(0.492/\mathrm{Pr})^{9/16}\right]^{8/27}}\right\}^2 \;\; for\; 10^{-1}<Ra_{l_{s,o}}<10^{12},$$
$$Ra_{l_{s,out}} = Gr_{l_{s,out}}\,\mathrm{Pr};\;\; Gr_{l_{s,out}} = \frac{g\,l_{io}^3\beta((\omega_w T_w + \omega_a T_a) - T_{so})}{\mu_a^2/\rho_a^2},\;\; \mathrm{Pr} = \frac{\mu_a\, cp_a}{k_a} \tag{21}$$

where k (W/mK) is the thermal conductivity, Pr (-) is Prandtl number, Ra (-) is Rayleigh number, h (W/m^2K) is the convective heat transfer coefficient, Gr (-) is Grashoff number, l(m) is the length or dimension of the bath, g(m/s^2) is the gravitational constant, β (1/K) is the temperature coefficient, and the thermophysical properties of the fluids found in Equations (17) and (19) are defined by mathematical correlation in Table 1 (Nnamchi et al., 2019).

3. Discussion and results

The presentation of results and subsequent discussion of the results is carefully articulated in this section (Section 3.0).

3.1. The input data

Essentially, Table 1 summarizes the TP of the heat transfer fluids employed in the experimentation and in computing the numerical values of the heat transfer fluids properties. The characteristic roots or eigenvalue of the transcendental equations in Equations (13) and (14) commensurate to the boundary conditions in Figure 2 have been solved by Ozisik (1993) for the first six roots. However, the results are made handy by transforming them into regression models in Table 2 for the wide range of ratio of convective heat transfer coefficient to the thermal conductivity of the material (mild steel pipe). The regression coefficient, R^2 in Table 2 portrays that there is strong correlation among the separation constants since R^2 is virtually unity for the models.

3.2. Results

Explicitly, Figures 7–10 present the experimental cooling results obtained from experimentation on the ITR. Significant change in temperature was observed every 3 min, thus, an interval of 3 min was employed throughout the experiment whereas Table 3 shows the input data employed in the analysis of the experimental results via Equations (1)–(21).

Table 1. Thermal properties of the working fluids (air and water) at the fluid temperature

S#	Parameter	Unit	Equation	
			Air (a)	Water (w)
1.	Temp. coefficient, β	$(1/K)$	$1/T_a$(or $1/T_w$)	$1/T_w$
2.	Density, ρ	kg/m^3	$\rho_a = 2.1313 - 0.003T_a$	$\rho_w = 754.3079871 + 1.881328437T_w - 0.00358317T_w^2$
3.	Viscosity, μ	$kg/m\,s$	$\mu_a = 1.03 \times 10^{-6} + 7 \times 10^{-8}\,T_a - 4 \times 10^{-11}\,T_a^2$	$\mu_w = 146039867076.91\,T_w^{-5.74}$
4.	Heat capacity, cp	$J/kg\,K$; $kJ/kg\,K^*$	$cp_a = 1031.31 - 0.2047\,T_a + 0.00042\,T_a^2$	$cp_w^* = 5.476 - 0.008178\,T_w + 0.000013T_w^2$
5.	Thermal cond., k	$W/m\,K$	$k_a = 0.0121e^{(0.0025\,T_a)}$	$k_w = 0.0223\,T_w^{0.5802}$
6.	Air speed, u	m/s	1.55	

Table 2. The separation constants of transcendental equation in Equation (12)

S#	Root of transcendental equation (λ)	Regression coefficient, R^2
1.	$\lambda_6 \approx 15.705980232456 + 0.069430947598\,(h/k) - 0.001647564096\,(h/k)^2 + 0.000021069658\,(h/k)^3 - 0.000000135856\,(h/k)^4 + 0.000000000345(h/k)^5$	1.0000
2.	$\lambda_5 \approx -51.833 + 6.9285\,\lambda_6 - 0.1801\,\lambda_6^2$	1.0000
3.	$\lambda_4 \approx -123.21 + 15.253\,\lambda_6 - 0.4335\,{\lambda_6}^2$	1.0000
4.	$\lambda_3 \approx -223.16 + 27.086\,\lambda_6 - 0.7944\,{\lambda_6}^2$	0.9978
5.	$\lambda_2 \approx Exp\left(-26.833 + 27.259\,\ln(\lambda_3) - 6.5473\,(\ln(\lambda_3))^2\right);\ \lambda_3 > 0$	0.9986
6.	$\lambda_1 \approx Exp\left[\begin{matrix} -0.1546 + 0.3514\,\ln(h/k) - 0.00496\,(\ln(h/k))^2 \\ -0.0042\,(\ln((h/k)))^3 + 0.0006\,(\ln(h/k))^4 + 0.00008\,(\ln(h/k))^5 \end{matrix}\right];\ h/k > 0$	1.0000

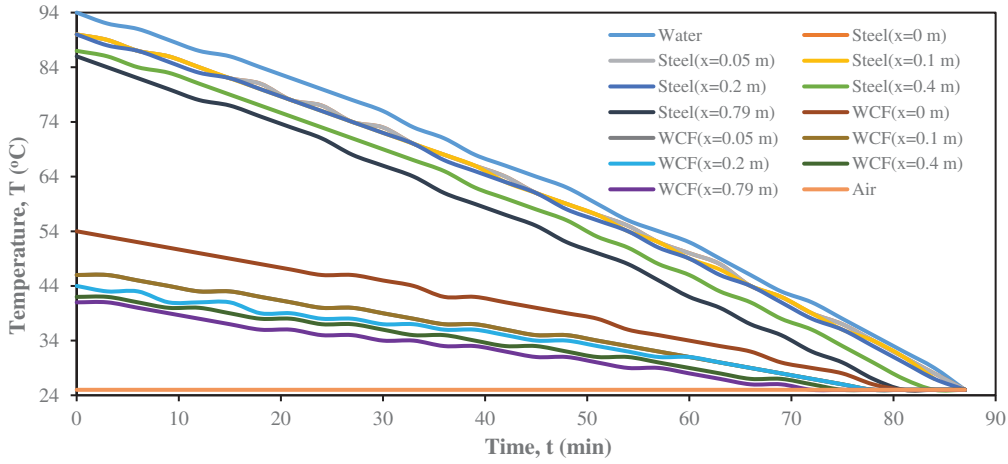

Figure 7. Measured temperature for white cotton fabric (WCF) insulating material, mild steel pipe (steel) and heat transfer fluids (air and water).

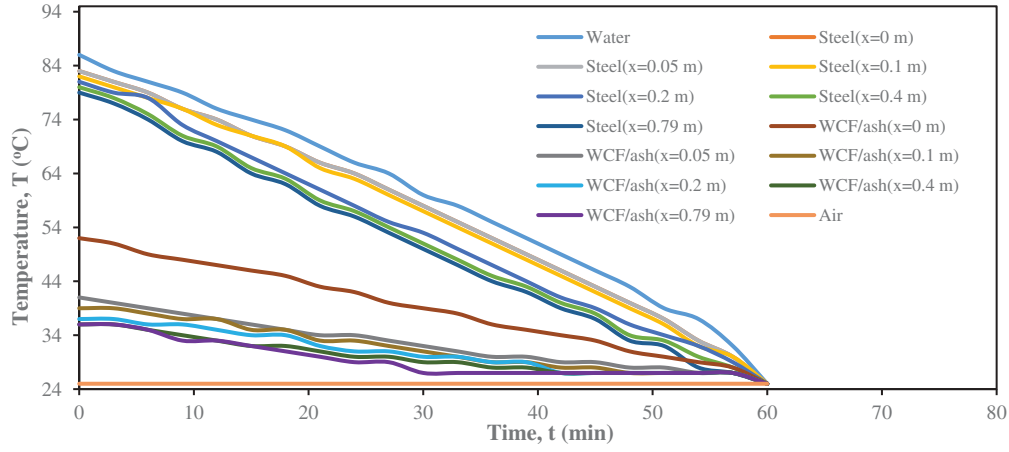

Figure 8. Measured temperature for WCF/molded ash insulating material, mild steel pipe (steel) and heat transfer fluids (air and water).

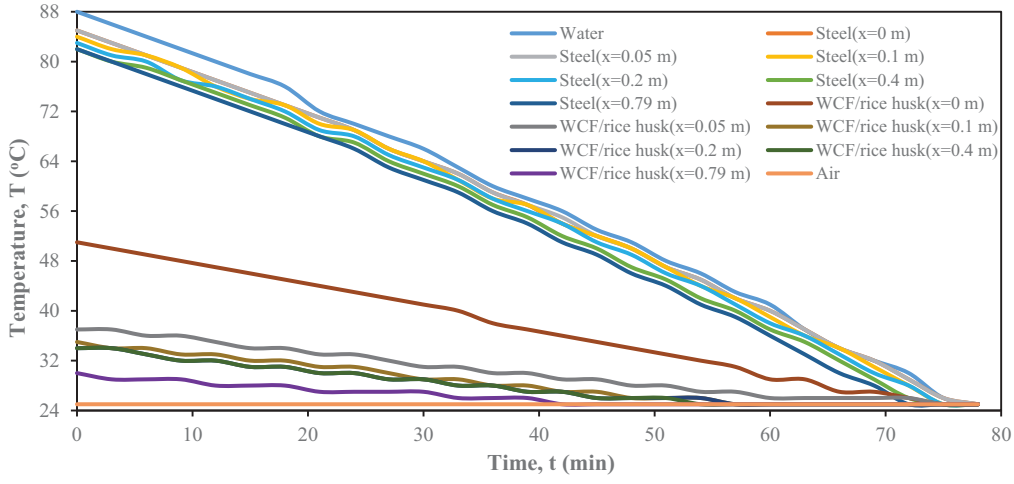

Figure 9. Measured temperature for WCF/molded rice husk insulating material, mild steel pipe (steel) and heat transfer fluids (air and water).

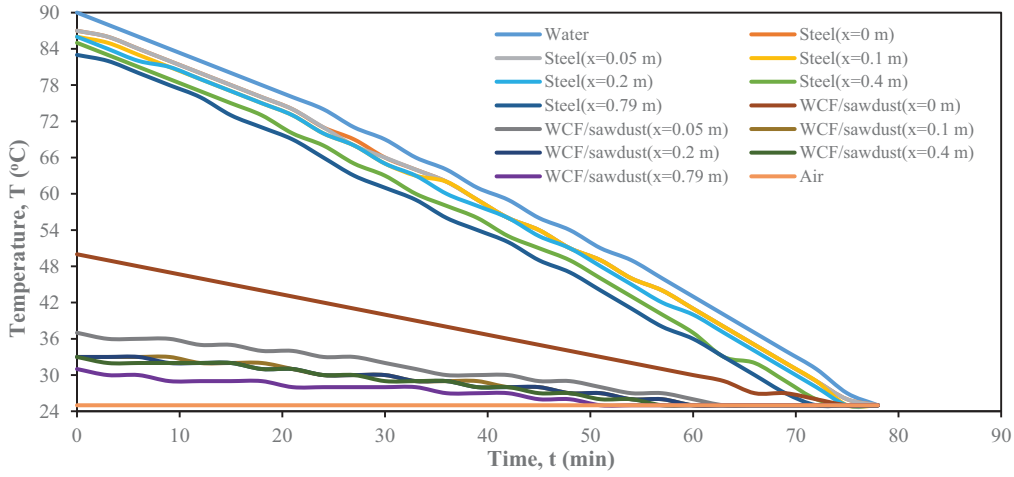

Figure 10. Measured temperature for WCF/molded sawdust insulating material, mild steel pipe (steel) and heat transfer fluids (air and water).

3.3. Discussion

The thermal rejection factor, $n_{i,j}$ in Figure 11 is translated into mathematical functions in Table 4 by adding trend line to the different sections of the curves in order to achieve regression coefficients of unity in all the sections ($0.0 \leq x \leq 0.79$). This parameter is vital for computing the thermal conductivity of the IM in Equations (9) and (10). However, the complexity in fitting the curves in Figure 11 was resolved by breaking them into three different sections ($x<0.1;0.1 \leq x \leq 0.2;x>0.2$) to have highest degree of fitting ($R^2 = 1$). Thus, the leading and tail sections were appropriately fitted with a quadratic function whereas the mid-section was properly fitted with a linear function in Figure 11. Generally, Figure 11 depicts that HRF decreases along the cylindrical test surface due to drop in thermal gradient along the cylindrical test surface. Experimentally, the molded sawdust insulating material exhibited a least thermal rejection factor compared to the other IM investigated. Unequivocally, this upshot could be attributed to the presence of lattice vibration wave or absence of phonon (a travelling wave) in the lattice of the molded sawdust whereas the rest of the IM tested, especially the white cotton fabric recorded thermal rejection factor of the highest order, which suggests that there is appreciable amount of phonon in its lattice. Therefore, HRF is certainly influenced by the magnitude of lattice vibration wave or energy and stands out as one of the criteria for selecting potential IM (A-wastes).

Conversely, Figure 12 gives an overview of effectiveness of the different IM being verified; it simply delineates the thermal retention potential or capability of the different IM. Consequently, the molded sawdust proved to be more effective relative to the other IM due to the fact that only lattice vibration wave is present in the material in a minute quantity. Also, the effectiveness builds up from the base to the end of the cylindrical test surface due to drop in the thermal gradient along the test surface of the ITR. The thermal conductivity of the IM were computed based on Equation (10), which is a function of the HRF, the geometric features of the mild steel cylindrical surface upon which the molded insulating material was laid on, and the heat transfer coefficients of heat transfer fluids.

Expectantly, Figure 13 portrays that low thermal conductivity in the molded IM correspond to low HRF, density and specific heat capacity, and partly due to the magnitude of the thermal agitation in the lattice of the IM, which supports Stabler et al. (2018) assertion. Conversely, Equation (11) shows that the thermal conductivity is inversely proportional to the insulation parameter of the molded IM, which is one of the indicators of sound IM. A good insulating material is characterized with high magnitude of insulation parameter, which could be attributed to low atomic vibration in the lattice of the insulating material.

Table 3. Input data for the analysis

		Monolith		Composite	
S#	**Parameter**	**WCF**	**WCF + molded ash**	**WCF + molded rice husk**	**WCF + molded sawdust**
1.	Dry weight of molded insulating materials, W (kg)	1.570	3.145 (0.102 + 3.043)	2.320 (0.102 + 2.218)	0.890 (0.102 + 0.788)
2.	Ambient temperature, T_a (°C)	25	25	25	25
3.	Bath temperature attained, T_w (°C)	94	86	90	90
4.	Base temperature for analysis, T_w (°C)	86	86	86	86
5.	Thermal conductivity of mild steel sheet, k_s (W/mK)	36.039	36.039	36.039	36.039
6.	Mild steel sheet thickness, δ_s (m)	0.00198	0.00198	0.00198	0.00198
7.	The outer radius of the pipe, $r_{s,out}$ (m)	0.03700	0.03700	0.03700	0.03700
8.	The inner radius of the pipe, $r_{s,in}$ (m)	0.03502	0.03502	0.03502	0.03502
9.	Insulating material thickness, δ_i (m)	0.0135	0.0130	0.0130	0.0130
10.	The inner radius of the insulating material, $r_{i,in}$ (m)	0.03700	0.03700	0.03700	0.03700
11.	The outer radius of the insulating material, $r_{i,out}$ (m)	0.0505	0.0500	0.0500	0.0500

(*Continued*)

Table 3. (*Continued*)

S#	Parameter	Monolith	Composite		
		WCF	**WCF + molded ash**	**WCF + molded rice husk**	**WCF + molded sawdust**
12.	Average wind velocity, u_w (m/s)	1.55	1.55	1.55	1.55
13.	Acceleration due to gravity (m/s^2)	9.81	9.81	9.81	9.81
14.	Dry weight powder and glue only: Powder→p, kg (glue→g, kg)	1.570 (0.000)	2.897 (0.145)	2.073 (0.145)	0.643 (0.145)

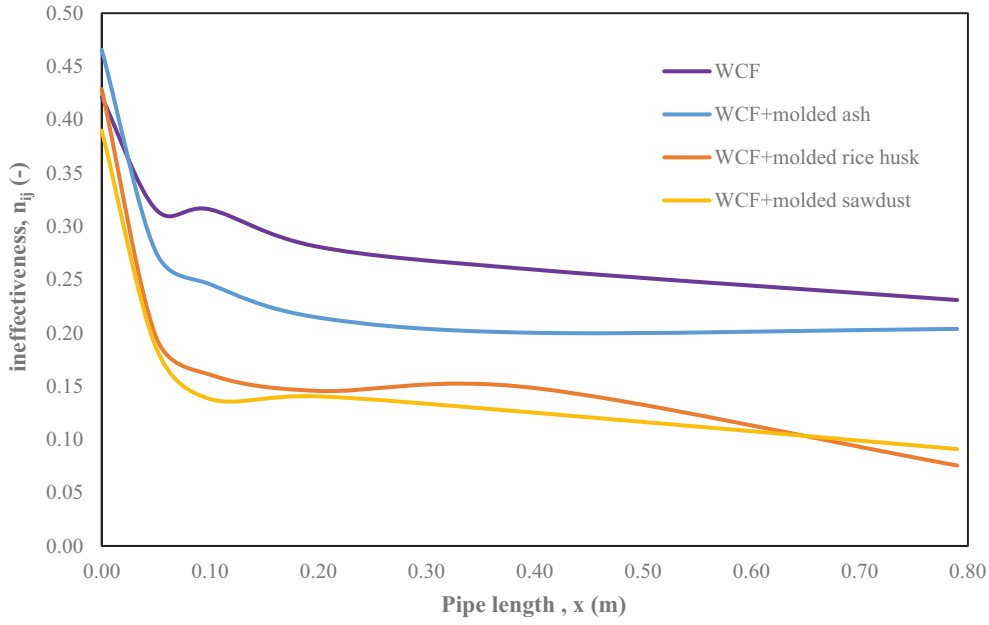

Figure 11. Thermal rejection factor for the unmolded/ molded insulating materials.

The analytical results of Equations (10) and (11) are presented in Tables 5 and 6, respectively. There are various published thermal conductivity results mentioned in the introductory section of this paper. However, the thermal conductivity of the white cotton fabric obtained from the ITR, 0.0597 W/mK was in very good agreement with the results, 0.0501 and 0.060 W/mK presented by Chidambaram, Govindan, and Venkatraman (2012), and Ozisik (1993), respectively. Moreover, the thermal conductivity of the molded ash from the ITR, 0.0377–0.0555 W/mK compared well with the results, 0.01–0.068 W/mK by Muia and Gaitho (2003). Furthermore, the thermal conductivity of molded rice husk from the ITR, 0.0251–0.0344 W/mK compared favorably with the result, 0.0359 by Kyauta et al. (2014). Also, the thermal conductivity of molded sawdust from the ITR, 0.0110–0.0293 W/mK compared well with the results, 0.030 and 0.059 W/mK by Karthikeyan et al. (2018) and Ozisik (1993), respectively. The unanimous and overwhelming agreement between the present results and established literature results buttress the fact that ITR is very good at presenting prominent and reliable results (thermal conductivity) of IM or potential A-wastes.

The present work has introduced insulation parameter in Table 6 for assessment or selection of IM from A-wastes. A high insulation parameter is an indication that a material has high thermal storage or low thermal conductance. A cross examination of the four IM verified the order of the insulation parameter: molded sawdust > molded rice husk > molded ash > WCF, these results correspond to the following order of the thermal conductivity; molded sawdust < molded rice husk < molded ash < WCF, respectively. Accordingly, the insulation parameter is inversely proportional to the thermal conductivity as supported by Equation (11).

where Also, the eigenvalues or the additive separation constants were computed and tabulated for the different insulating material. Observing Table 6 shows that the eigenvalues increases with the insulation parameter. This is obvious in order to maintain constant stabilization or equilibrium temperature (λ^{Γ}/m_i) in computing the thermal diffusivity. The external (forced) and the internal (free) convection were maintained constant in order to have equal basis for comparing the effectiveness of the IM in retaining heat.

Figures 14–17 present, a plot of the function, y (m^2), which is the ratio of dimensionless excess temperature to the insulation parameter against the cooling time, t (s) for the four different materials investigated. The curves were fitted with trend lines to obtain equation of fit for the

Table 4. Insulating material(s) thermal rejection factor, $n_{i,j}(x)$

Insulating material, i,j	Equation	Range	Regression coefficient, R^2 (-)
White cotton fabric (WCF)	$n_{i,j}(x) = 0.4211 - 3.1579x + 21.053x^2$	$x<0.1$	1.0000
	$n_{i,j}(x) = 0.3509 - 0.3509x$	$0.1 \leq x \leq 0.2$	1.0000
	$n_{i,j}(x) = 0.3068 - 0.142x + 0.0579x^2$	$x>0.2$	1.0000
WCF & molded ash (g + p)	$n_{i,j}(x) = 0.4655 - 5.3872x + 31.881x^2$	$x<0.1$	1.0000
	$n_{i,j}(x) = 0.2769 - 0.3133x$	$0.1 \leq x \leq 0.2$	1.0000
	$n_{i,j}(x) = 0.2395 - 0.1537x + 0.1372x^2$	$x>0.2$	1.0000
WCF & molded rice husk (g + p)	$n_{i,j}(x) = 0.4286 - 6.6071x + 39.286x^2$	$x<0.1$	1.0000
	$n_{i,j}(x) = 0.176 - 0.1526x$	$0.1 \leq x \leq 0.2$	1.0000
	$n_{i,j}(x) = 0.1157 + 0.2167x - 0.3387x^2$	$x>0.2$	1.0000
WCF & molded sawdust (g + p)	$n_{i,j}(x) = 0.3898 - 5.6166x + 30.976x^2$	$x<0.1$	1.0000
	$n_{i,j}(x) = 0.1355 + 0.0242x$	$0.1 \leq x \leq 0.2$	1.0000
	$n_{i,j}(x) = 0.1543 - 0.0659x - 0.0181x^2$	$x>0.2$	1.0000

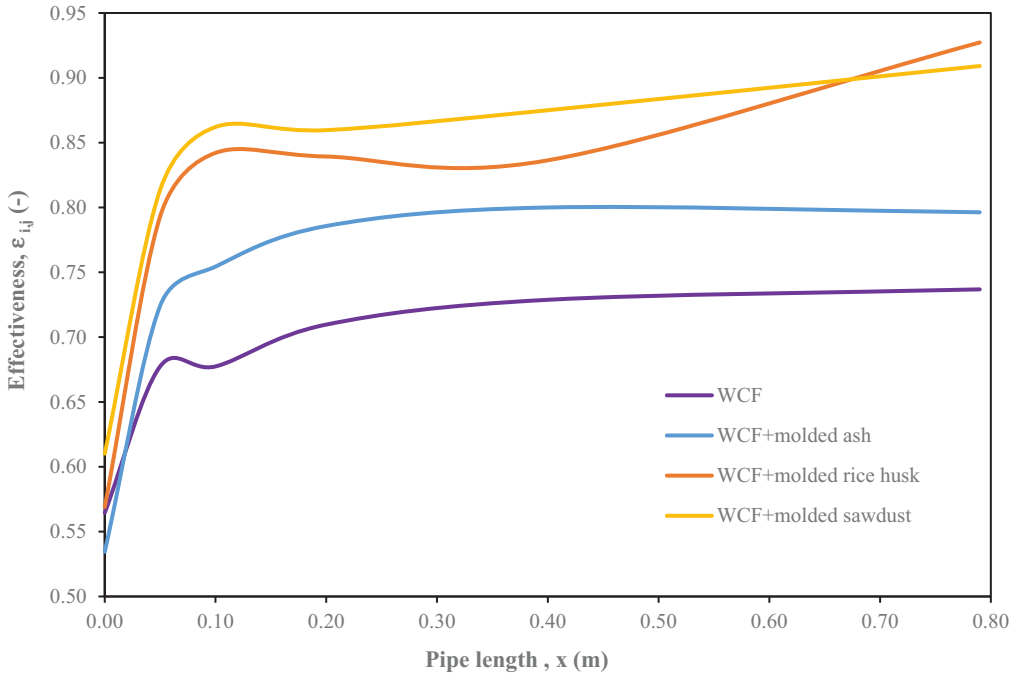

Figure 12. Thermal retention potential for the unmolded/ molded insulating materials.

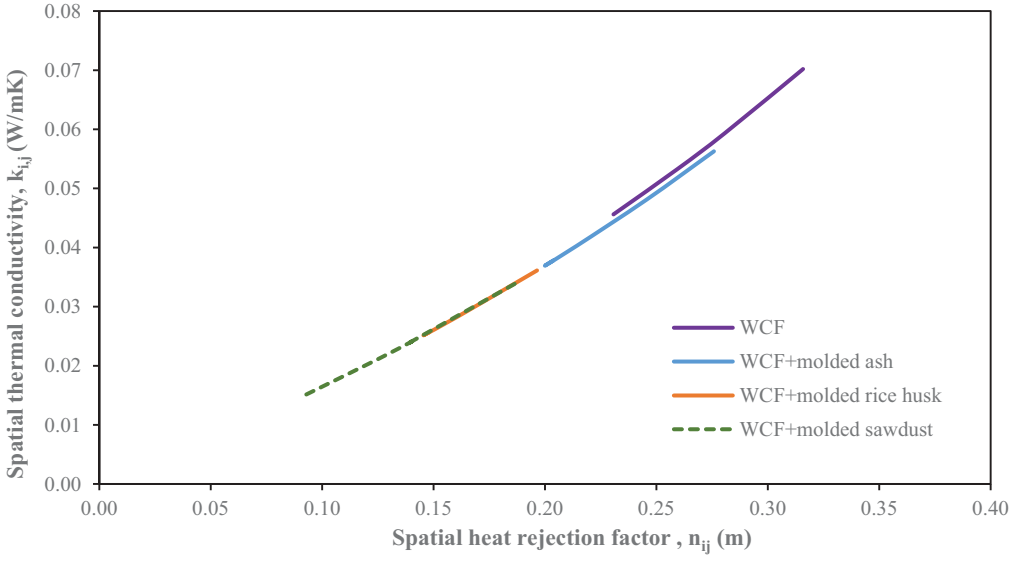

Figure 13. Dependency of thermal conductivity on the heat rejection factor for the different molded insulating materials.

different range of the insulation parameters (the lower and upper limits). Figures 14–17 portray the inverse relation between the insulation parameter and the thermal diffusivity; thus, the higher the insulation parameter, the lower the thermal diffusivity, thermal conductivity, specific heat and the density of the insulating material and vice versa.

The function y (m^2) is differentiated with respect to t (s) to obtain a slope (*dy/dt*) for the interval $0 \leq t \leq \infty$. Notably, the slopes of the curves in Table 7 correspond to the thermal diffusivities of the molded IM. The techniques is quite novel when compared to the popular method of comparing the thermal conductivity against the thermal storage ability of the IM in determining the thermal diffusivity.

Table 5. Computed range/average thermal conductivity (k) for the insulating materials

Insulating material	%wt of WCF	%wt of molded powder	Range: Dry composite k	Average: Dry composite k	Range: Molded powder k	Average: Molded powder k	Monolithic literature value
i	ω_{wcf} (-)	ω_{g+p} (-)	$k_{wcf+g+p}$(W/mK)	$\bar{k}_{wcf+g+p}$(W/mK)	k_{g+p} (W/mK)	$\bar{k}_{g+p}$ (W/mK)	k_p (W/mK)
WCF	1.000	0.000	0.046–0.070	0.0597	0.0597	0.0597	0.0501[a]; 0.06 [e]
WCF & molded ash (g + p)	0.032	0.968	0.038–0.056	0.0439	0.0377–0.0555	0.0434	0.01[b]–0.068[b]
WCF & molded rice husk (g + p)	0.044	0.956	0.026–0.036	0.0282	0.0251–0.0344	0.0268	0.0359[c]
WCF & molded sawdust (g + p)	0.115	0.885	0.015–0.034	0.0235	0.0110–0.0293	0.0188	0.030[d]; 0.059[e]

[a]Chidambaram et al. (2012), [b]Muia and Gaitho (2003), [c]Kyauta et al. (2014), [d]Karthikeyan et al. (2018), [e]Ozisik (1993).

Table 6. Essential parameters used for determining the thermophysical properties of the molded insulating materials

Insulating material, *i*	Range: Insulation parameter, m_i (1/m)	Average: Insulation parameter, $\bar{m}_i$ (1/m)	Characteristic root, λ^r (K/m^2)	Convective heat transfer coefficient (W/m^2K)	
				External, h_a	Internal, h_w
WCF	127.84–158.59	140.031	4.11–4.60	11.3600	935.0068
WCF & molded ash (g + p)	145.47–177.51	166.372	4.36–4.85	11.3600	935.0068
WCF & molded rice husk (g + p)	181.57–215.25	206.964	4.92–5.44	11.3600	935.0068
WCF & molded sawdust (g + p)	187.57–283.85	231.116	5.01–6.59	11.3600	935.0068

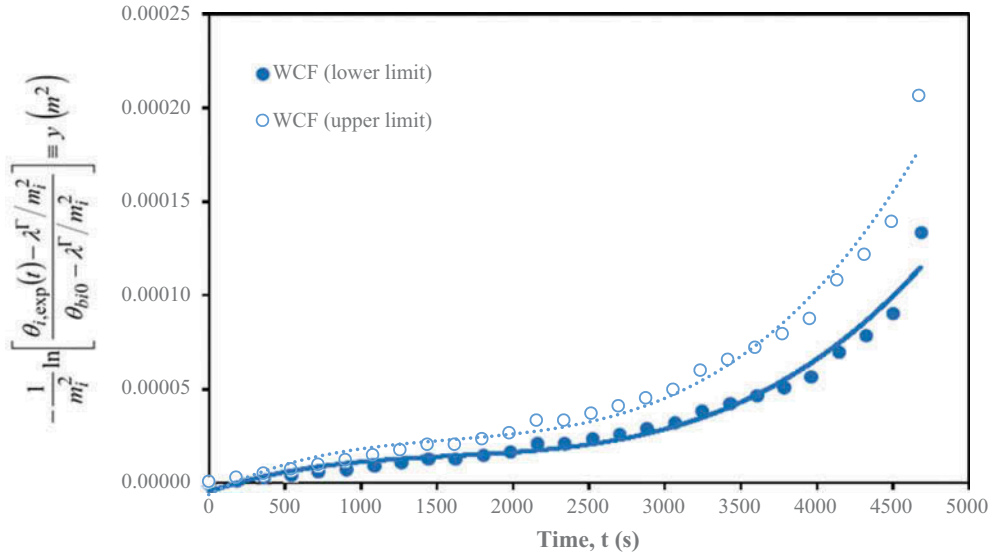

Figure 14. Derivation of thermal diffusivity of white cotton fabric insulating material.

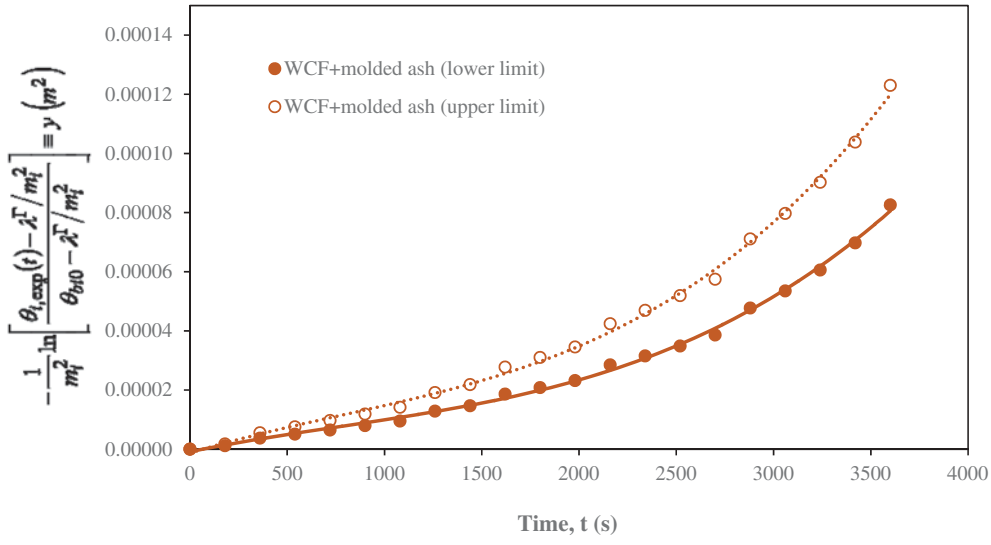

Figure 15. Derivation of thermal diffusivity of white cotton fabric and molded ash insulating materials.

The present work gives the range of thermal diffusivity for the different IM in Table 7 as; 2.712–4.174, 1.346–2.002, 1.112–1.562 and 0.533–1.222 m^2/s for the WCF, molded ash, molded rice husk and molded, respectively. Whereas Table 8 presents the thermal diffusivity of the molded IM (and the average thermal diffusivity) of WCF as 3.443×10^{-8} (3.443×10^{-8} m^2/s), which is in strong good agreement with the upper limit result, 3.41×10^{-8} m^2/s by Uzun (2014). Likewise, the present work presented the range of thermal diffusivity of the molded ash as $1.3008–1.9302 \times 10^{-8}$ (1.6155×10^{-8} m^2/s) this result is in good agreement with that of Ayugi et al. (2011), 3.67×10^{-8} m^2/s. Similarly, the present work furnished a range of thermal diffusivity of the molded rice husk as $1.0384–1.4418 \times 10^{-8}$ (1.2401×10^{-8} m^2/s) which compared very well with the result, $0.934–1.21 \times 10^{-8}$ m^2/s by Sreenarayanan and Chattopadyay (1986). Equally, the present work provided a range of thermal diffusivity of the molded sawdust as $0.2499–0.8384 \times 10^{-8}$ (0.54415×10^{-8} m^2/s) which is in good agreement with the dual results; 0.082 and 1.12×10^{-8} m^2/s by Engineers Edge (2019) and Ayugi et al. (2011), respectively.

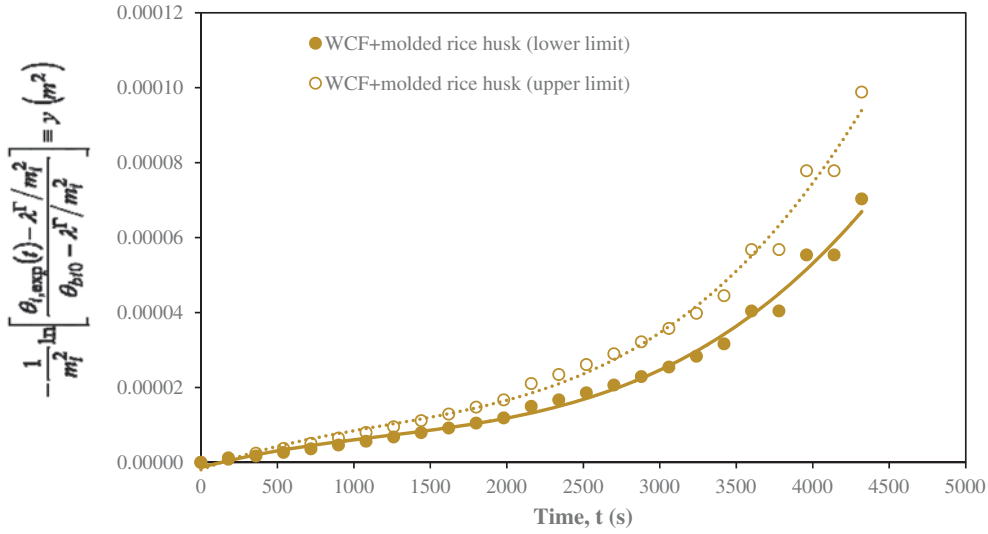

Figure 16. Derivation of thermal diffusivity for white cotton fabric and molded rice husk insulating materials.

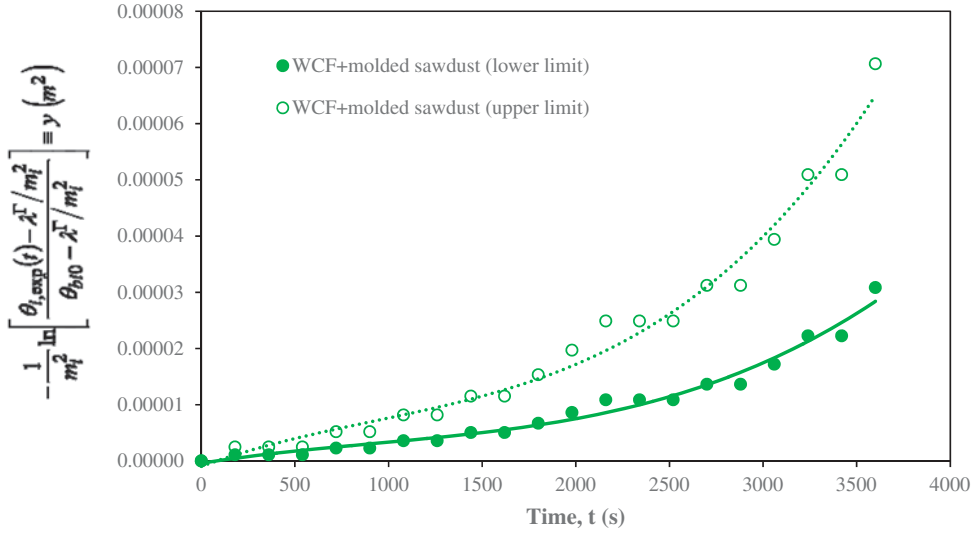

Figure 17. Derivation of thermal diffusivity of white cotton fabric and molded sawdust insulating materials.

Consequently, the agreement between the present work which is application of excess dimensionless temperature and insulation parameter in determining the thermal diffusivity against the traditional method which is application of the thermal conductivity and thermodynamic thermal storage capacity in determining the thermal conductivity of an insulating material and in recommendation of potential A-wastes as an insulating material. Thus, the agreement on the experimentally established thermophysical properties; the HRF, thermal conductivity, insulation parameter and thermal diffusivity support the fact that ITR reliable equipment for verification of the thermophysical properties of IM.

4. Conclusion

Experimental verification of suitability of ITR in determining the thermophysical properties of IM has been carried out via four thermophysical properties; the HRF (dimensionless excess temperature), thermal conductivity, insulation parameter and thermal diffusivity. These cardinal thermophysical properties were extended to four different IM and the range of results experimentally orchestrated, unanimously agreed with the existing literature results.

Table 7. Computed thermal diffusivity of the composite insulating materials

Insulating material	Equation	slope	α_{c+g+p} x10^8 (m^2/s)
WCF	$y = 3.0 \times 10^{-15}t^3 \ -1.42675 \times 10^{-11}t^2 + 2.7119254 \times 10^{-8}t$ -0.0000046101485575 $y = 4.6 \times 10^{-15}t^3 \ - 2.19574 \times 10^{-11}t^2 + 4.17356452 \times 10^{-8}t \ -0.0000070949622479$	$dy/dt = 9.0 \times 10^{-15}t^2 - 4.95812 \times 10^{-11}t + 2.7119254 \times 10^{-8} = 0$ $dy/dt = 9.2 \times 10^{-15}t^2 - 4.39148 \times 10^{-11}t + 4.17356452 \times 10^{-8} = 0$	2.712–4.174
WCF & molded ash (g + p)	$y = 2.0 \times 1$ $0^{-15}t^3 \ - 4.6491 \times 10^{-12}t^2 + 1.34455302 \times 10^{-8}t - 0.000000856821414573$ $y = 3.0 \times 10^{-15}t^3 \ - 6.92295 \times 10^{-12}t^2 + 2.0021165 \times 10^{-8}t - 0.0000012758882573$	$dy/dt = 6 \times 10^{-15}t^2 - 9.2982 \times 10^{-12}t + 1.34455302 \times 10^{-8} = 0$ $dy/dt = 9.0 \times 10^{-15}t^2 - 1.38459 \times 10^{-12}t + 2.0021165 \times 10^{-8} = 0$	1.346–2.002
WCF & molded rice husk (g + p)	$y = 1.4 \times 10^{-15}t^3 - 5.1365 \times 10^{-12}t^2 + 1.11163898 \times 10^{-8}t$ $-0.0000013882403847 = 0.0000000000000020t^3$ $-0.0000000000056531t^2 + 0.0000000122185458t$ -0.0000009582477136 $y = 2.0 \times 10^{-15}t^3 \ - 7.2191 \times 10^{-12}t^2 + 1.5623151 \times 10^{-8}t \ - 0.0000019510803365$	$dy/dt = 4.2 \times 10^{-15}t^2 - 1.0273 \times 10^{-11}t + 1.11163898 \times 10^{-8} = 0$ $dy/dt = 6.0 \times 10^{-15}t^2 - 1.44382 \times 10^{-11}t + 1.5623151 \times 10^{-8} = 0$	1.112–1.562
WCF & molded sawdust (g + p)	$y = 9.0 \times 10^{-16}t^3 \ - 2.4681 \times 10^{-12}t^2 + 5.3347692 \times 10^{-9}t$ -0.0000004183633939 $y = 6.0 \times 10^{-15}t^3 \ - 5.6531 \times 10^{-12}t^2 + 1.22185458 \times 10^{-8}t \ - 0.0000009582477136$	$dy/dt = 2.7 \times 10^{-15}t^2 - 4.9362 \times 10^{-12}t + 0.53347692 \times 10^{-8} = 0$ $dy/dt = 4.0 \times 10^{-15}t^2 - 1.13062 \times 10^{-11}t + 1.22185458 \times 10^{-8} = 0$	0.533–1.222

cogent engineering

Table 8. Computed thermal diffusivity (α) of the molded insulating materials

Insulating material	%wt of WCF	%wt of molded powder	Range: Dry composite α	Average: Dry composite α	Range: Molded powder α	Average: Molded powder α	Monolithic literature value
i	ω_{wcf} (-)	ω_{g+p} (-)	$\alpha_{wcf+g+p} \times 10^8$ (m^2/s)	$\bar{\alpha}_{wcf+g+p} \times 10^8$ (m^2/s)	$\alpha_{g+p} \times 10^8$ (m^2/s)	$\bar{\alpha}_{g+p} \times 10^8$ (m^2/s)	$\alpha_p \times 10^8$ (m^2/s)
WCF	1.000	0.000	2.712–4.174	3.443	3.443	3.443	0.86 [e]–3.41 [e]
WCF & molded ash (g + p)	0.032	0.968	1.346–2.002	1.674	1.3008–1.9302	1.6155	3.67[g]
WCF & molded rice husk (g + p)	0.044	0.956	1.112–1.562	1.337	1.0384–1.4418	1.2401	0.934[h]–1.21[h]
WCF & molded sawdust (g + p)	0.115	0.885	0.533–1.222	0.8775	0.2499–0.8384	0.54415	0.082[f], 1.12[g]

where [e]Uzun (2014), [f]Engineers Edge (2019), [g]Ayugi et al. (2011), [h]Sreenarayanan and Chattopadyay (1986)

The contribution to the state-of-art was made by the introduction of additional thermophysical properties; the HRF (dimensionless excess temperature) and insulation parameter alongside with the traditional thermophysical properties used in characterization of IM.

Appropriately, the thermal conductivity was determined as the function of HRF, regular geometric shapes of the mild steel cylindrical test surface and the IM and convective heat transfer coefficient of the heat transfer fluids.

Distinctively, the insulation parameter was determined as the ratio of the product of the external conductance around the insulating material and perimeter of the insulating material to the product of thermal conductivity (internal conductance within the insulating material) and the cross-sectional area of the insulating material available to the conductive thermal flux. Innovatively, the thermal diffusivity was determined as the ratio of the product of the rate of dimensionless excess temperature over the insulating material and the insulation parameter of the insulation material. The feasible thermal conductivity for the white cotton fabric, molded ash, molded rice husk and molded sawdust IM are; 0.0597, 0.0377–0.0555, 0.0251–0.0344 and 0.0110–0.0293 W/mK, respectively. Similarly, the thermal diffusivity obtained for the above-mentioned IM are; 3.443, 1.3008–1.9302, 1.0384–1.4418 and 0.2499–0.8384 m^2/s, respectively.

Moreover, the results obtained with the innovative thermophysical properties; the thermal conductivity and diffusivity were in good agreement with the similar ones obtained from the traditional techniques. Hence, the experimental verification of ITR was successfully carried out and the experimental results substantiate that ITR is germane for the verification of thermophysical properties of other A-wastes as a meaningful extension of this work.

Acknowledgements
The authors wish to acknowledge the Management of Kampala International University for providing the necessary research facilities used in this work.

Funding
The authors received no direct funding for this research.

Author details
S. N. Nnamchi[1]
E-mail: stephen.nnamchi@kiu.ac.ug
ORCID ID: http://orcid.org/0000-0002-6368-2913
O. A. Nnamchi[2]
E-mail: onyxhoni@yahoo.com
ORCID ID: http://orcid.org/0000-0003-4099-601X
O. S. Odebiyi[1]
E-mail: samuel.oluwasegun@kiu.ac.ug
O. O. Edosa[1]
E-mail: osaruene@kiu.ac.ug
ORCID ID: http://orcid.org/0000-0001-8241-3455
T. Wanazusi[1]
E-mail: titus.wanasusi@studmc.kiu.ac.ug
ORCID ID: http://orcid.org/0000-0003-1334-9503
[1] Department of Mechanical Engineering, SEAS, Kampala International University, Ggaba Road, Kansanga, P.O.B, Kampala 20000, Uganda.
[2] Department of Agricultural Engineering and Bio Resources, Michael Okpara University of Agriculture, Umudike, Umuahia, Nigeria.

Disclosure statement
No potential conflict of interest was reported by the authors.

Citation information
Cite this article as: Experimental verification of suitability of insulation testing rig in determining thermophysical properties of insulating materials, S. N. Nnamchi, O. A. Nnamchi, O. S. Odebiyi, O. O. Edosa & T. Wanazusi, *Cogent Engineering* (2019), 6: 1657264.

References

Ayugi, G., Banda, E. J. K. B., & D'Ujanga, F. M. (2011). Local thermal insulating materials for thermal energy storage. *Rwanda Journal of Mathematical Sciences, Engineering and Technology*, *23*(Series C), 21–29.

Balaguru, R. J. B., & Jeyaprakash, B. G. (2019). Lattice vibrations, phonons, specific heat capacity, thermal conductivity. *NPTEL – Electrical & Electronics Engineering – Semiconductor Nanodevices*. SASTRA University. Retrieved from www.nptel.ac.in/courses/115106076/Module%209/Module%209.pdf

Behnia, K., & Kapitulnik, A. (2019). A lower bound to the thermal diffusivity of insulators. *Journal of Physics: Condensed Matter*, *31*(40), 8953–8984.

Chidambaram, P., Govindan, R., & Venkatraman, K. C. (2012). Study of thermal comfort properties of cotton/regenerated bamboo knitted fabrics. *African Journal of Basic & Applied Sciences*, *4*(2), 60–66. doi:10.5829/idosi.ajbas.2012.4.2.1032

Ebiega, E. O. (2017). *Investigation of the thermal properties of wood ash and clay-sawdust mixture for use as insulation materials in a rocket stove* (M.Eng Thesis). ABU, Nigeria.

Engineers Edge. (2019). Thermal diffusivity table, heat transfer engineering and design. Retrieved from www.engineersedge.com/heat_transfer/thermal_diffusivity_table_13953.htm

Guo, P., & Feng, M. (2011). A research on performance of waste polystyrene insulation block. *Advanced Material Research Journal Advanced in Building Materials*, *168–170*, 1055–1060.

Karthikeyan, N., Manapparai, M., Prabu, M., & Ekanthamoorthy, J. (2018). Investigate the thermal conductivity of insulating powders. *International Journal of Latest Technology in Engineering, Management & Applied Science (IJLTEMAS)*, *7*(6), 2278–2540.

Kreith, F. (2000). *The CRC handbook of thermal engineering* (pp. 33431). Boca Raton, Florida: CRC Press LLC, Corporate Blvd., N.W.

Kuye, A. O., Oko, C. O. C., & Nnamchi, S. N. (2010). Determination of the thermal conductivity and specific heat capacity of neem seeds by inverse problem method. *Journal of Engineering Science and Technology Review*, *3*(1), 1–6. doi:10.25103/jestr

Kyauta, E. E., Dauda, D. M., & Justin, E. (2014). Investigation on thermal properties of composite of rice husk, corncob and baggasse for building thermal insulation. *American Journal of Engineering Research (AJER)*, *3*(12), 34–40.

Muia, L. M., & Gaitho, F. (2003). Thermal conductivity of wood ash diatomite composites using the transient hot strip method (IC/IR–2003/14). *International Atomic Energy Agency (IAEA)*. Retrieved from https://inis.iaea.org/collection/NCLCollectionStore/_Public/35/024/35024578.pdf?r=1&r=1

Nnamchi, S. N., Nnamchi, O. A., Sangotayo, E. O., Mundu, M. M., & Edosa, O. O. (2019). Design and fabrication of insulation testing rig. *Indian Journal of Engineering*, *16*, 60–79.

Nnamchi, S. N., Sanya, O. D., Zaina, K., & Gabriel, V. (2018). Development of dynamic thermal input models for simulation of photovoltaic generators. *International Journal of Ambient Energy*, 1–13. doi:10.1080/01430750.2018.1517676

Oko, C. O. C. (2008). *Engineering thermodynamics: An algorithmic approach*. Port Harcourt, Nigeria: University of Port Harcourt Press.

Oko, C. O. C. (2011). *Introduction to heat transfer: an algorithmic approach* (2nd ed.). Port Harcourt, Nigeria: University of Port Harcourt Press.

Ozisik, N. M. (1993). *Heat conduction*. New York: John Wiley & Sons Inc.

Rajput, R. K. (2007). *Engineering thermodynamics* (3rd ed, S.I. unit version). New Delhi: LAXMI Publications (P) LTD.

Schilling, A., Zhang, X., & Bossen, O. (2019). Heat flowing from cold to hot without external intervention by using a “thermal inductor. *Science Advances*, *5*(4), eaat9953. doi:10.1126/sciadv.aat9953

Sreenarayanan, V. V., & Chattopadyay, P. K. (1986). Thermal conductivity and diffusivity of rice bran. *Journal of Agricultural Engineering Research*, *34*(2), 115–121. doi:10.1016/S0021-8634(86)80004-X

Stabler, C., Reitz, A., Stein, P., Albert, B., Riedel, R., & Ionescu, E. (2018). Thermal properties of SiOC glasses and glass ceramics at elevated temperatures. *Materials*, *11*(2), 279. doi:10.3390/ma11020279

Uzun, M. (2014). Characterisation of thermal diffusivity and tensile properties of ultrasonically washed woven fabrics. *QScience Connect*, *2014*, 2.

Yüksel, N. (2016). *The review of some commonly used methods and techniques to measure the thermal conductivity of insulation materials*. Intech Open publisher. doi:10.5772/64157

Zhu, W., Wu, G., Chen, H., & Ren, J. (2018). Nonlinear heat radiation induces thermal rectifier in asymmetric holey composites. *Frontiers in Energy Research*, *6*. doi:10.3389/fenrg.2018.00009

***Cogent Engineering* (ISSN: 2331-1916) is published by Cogent OA, part of Taylor & Francis Group.**